Electronic Supplementary Material (ESI) for Dalton Transactions.

Supporting Information

Di- and Tetranuclear Transition Metal Complexes of a Tetrakisguanidino-Substituted Phenazine Dye by Stepwise Coordination

Roxana Lorenz, Elisabeth Kaifer, Hubert Wadepohl, Hans-Jörg Himmel*

Comparison between the results from TD-DFT calculations and the measured UV/Vis spectra as well as assignment of the lowest-energy electronic transitions

a) b)

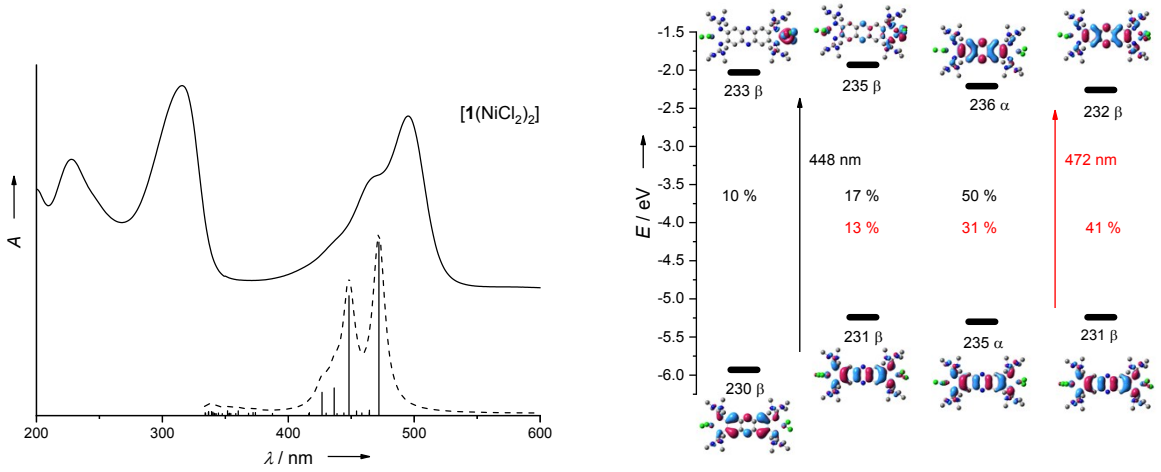

Figure S1 a) Comparison between the experimentally obtained electronic absorption spectrum for [**1**$(NiCl_2)_2$] dissolved in CH_3CN solution (—) and a simulation (- - -) based on a TD-DFT calculation at the B3LYP-D3/def2-TZVP level; b) Isodensity surfaces of the orbitals contributing to the two most-intense bands at 448 (black) and 472 nm (red).

a) b)

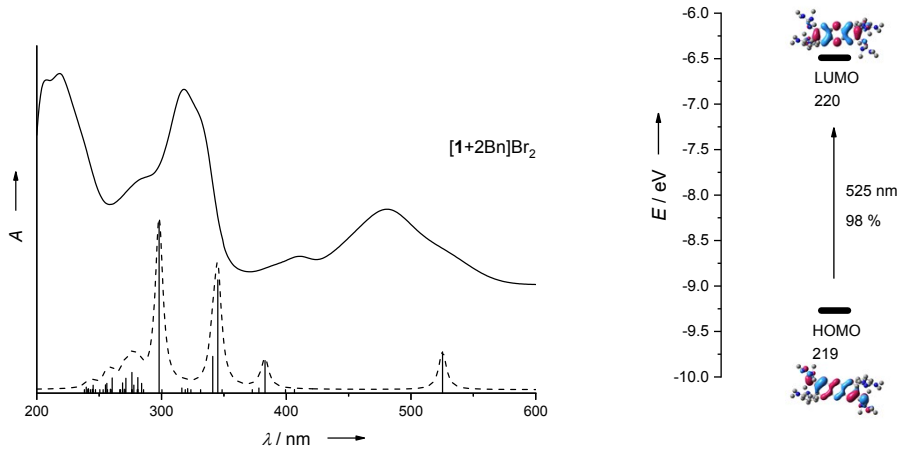

Figure S2 a) Comparison between the UV/Vis spectrum for [**1**+2Bn]Br_2 in CH_3CN solution (—) and a simulation (- - -) based on TD-DFT calculations at the B3LYP-D3/def2-TZVP level; b) Isodensity surfaces of the orbitals contributing to the band at 525 nm.

a) b)

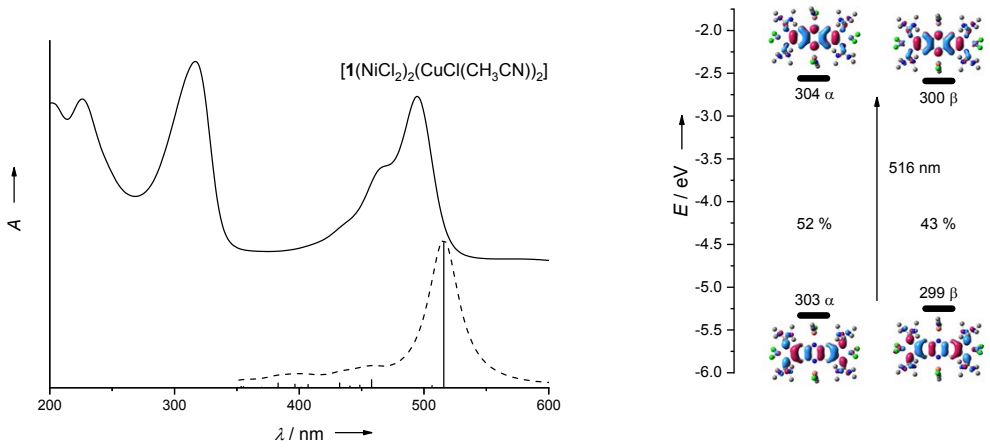

Figure S3 a) Comparison between the UV/Vis spectrum of [**1**$(NiCl_2)_2(CuCl(CH_3CN))_2$] in CH_3CN solution (—) and a simulation (- - -) based on a TD-DFT calculations on the B3LYP-D3/def2-TZVP level. b) Isodensity surfaces of the orbitals contributing to the band at 516 nm.

Photos of solutions of **1**, [**1**$(CuCl_2)_2$], [**1**$(NiCl_2)_2$] and [**1**+2Bn]Br_2 (from left to right) in CH_3CN.

Analytical data for all compounds

EPR spectra for [1(CuCl$_2$)$_2$]

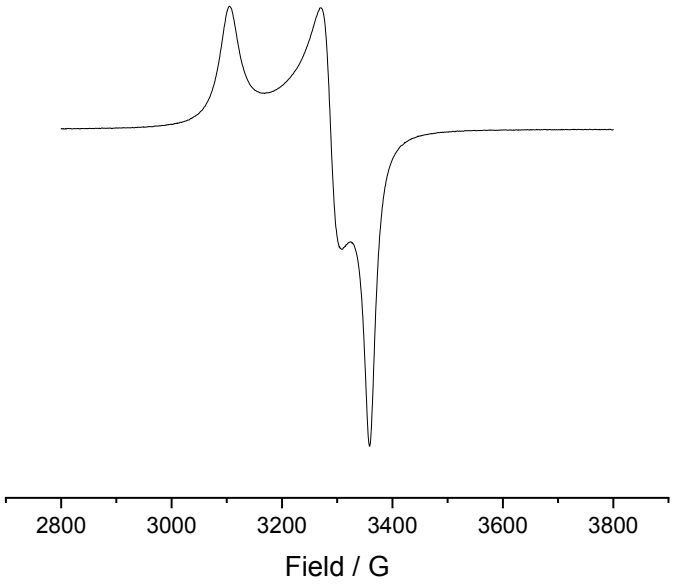

Figure S4 EPR-spectrum (RT, solid): g_1 = 2.216, g_2 = 2.096, g_3 = 2.057 (ν = 9.638289 GHz).

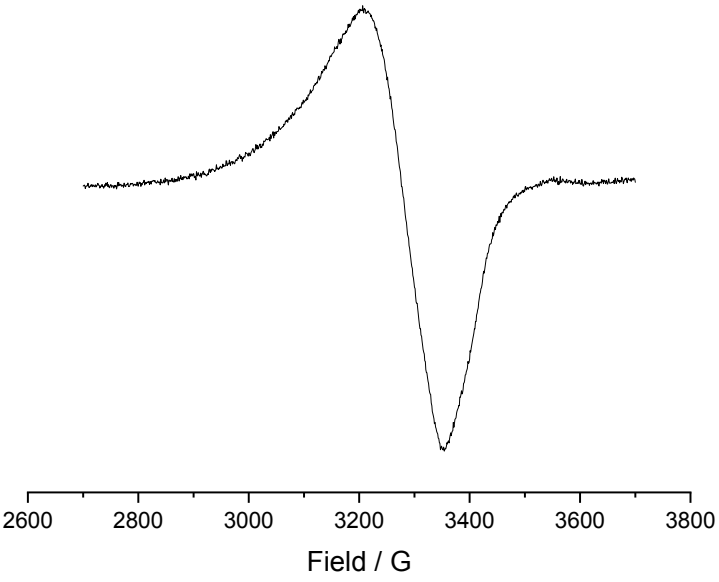

Figure S5 EPR-spectrum (RT, CH_2Cl_2 solution): g = 2.120 (ν = 9.63795 GHz).

Absorption and emission spectra for 1

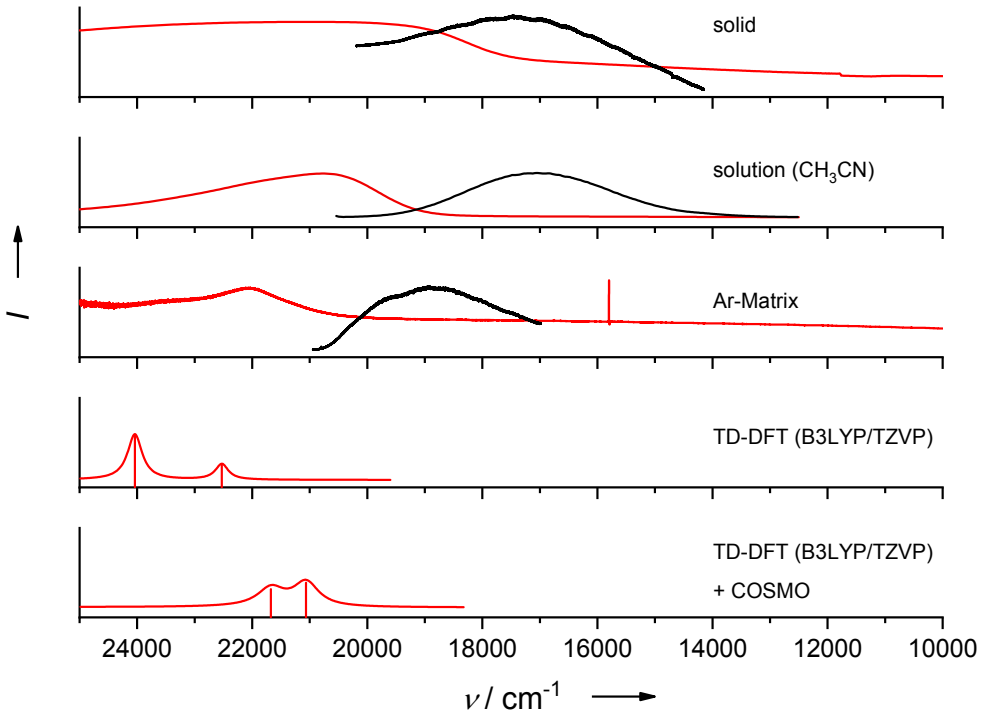

Figure S6 Electronic absorption (red) and emission (black) spectra for **1** in the solid material, in CH_3CN solution, in an Ar matrix (4 K) as well as calculated (B3LYP/TZVP) absorption spectra without and with simulation of the solvent effect by COSMO (ε_r = 37.5).

Analytical data for [1+2R]Br_2

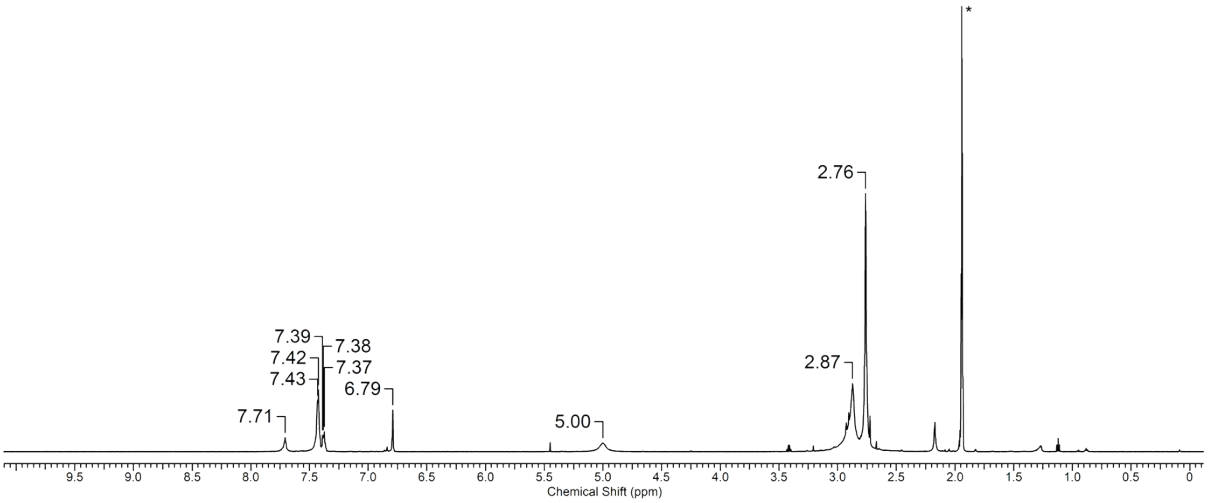

Figure S7 ^{1}H NMR spectrum (600 MHz) of [**1**+2Bn]Br_2 dissolved in CD_3CN.

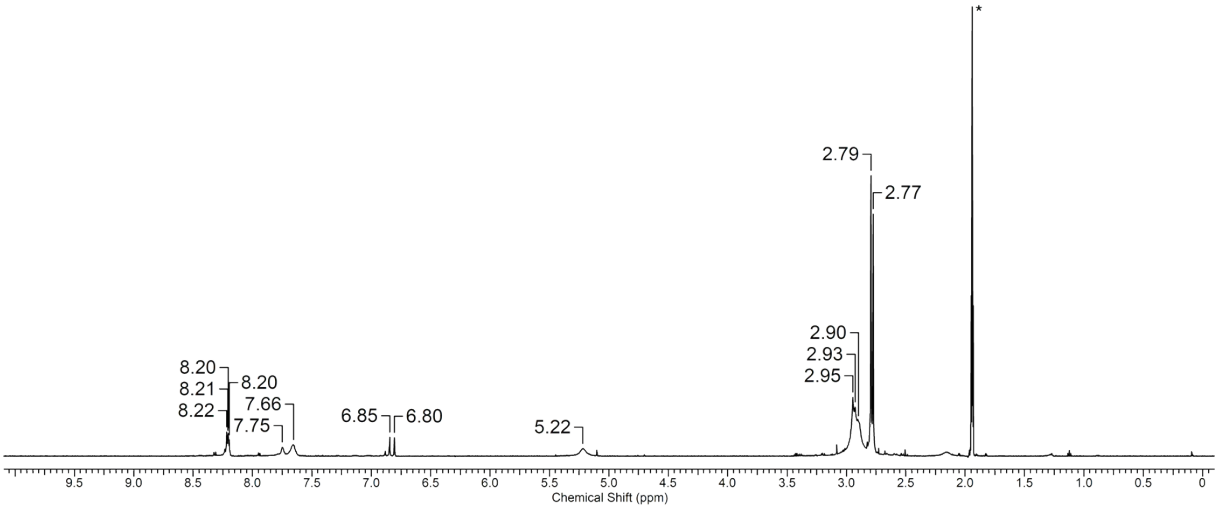

Figure S8 ^{1}H NMR spectrum (600 MHz) of [**1**+2(p-NO_2Bn)]Br_2 dissolved in CD_3CN.

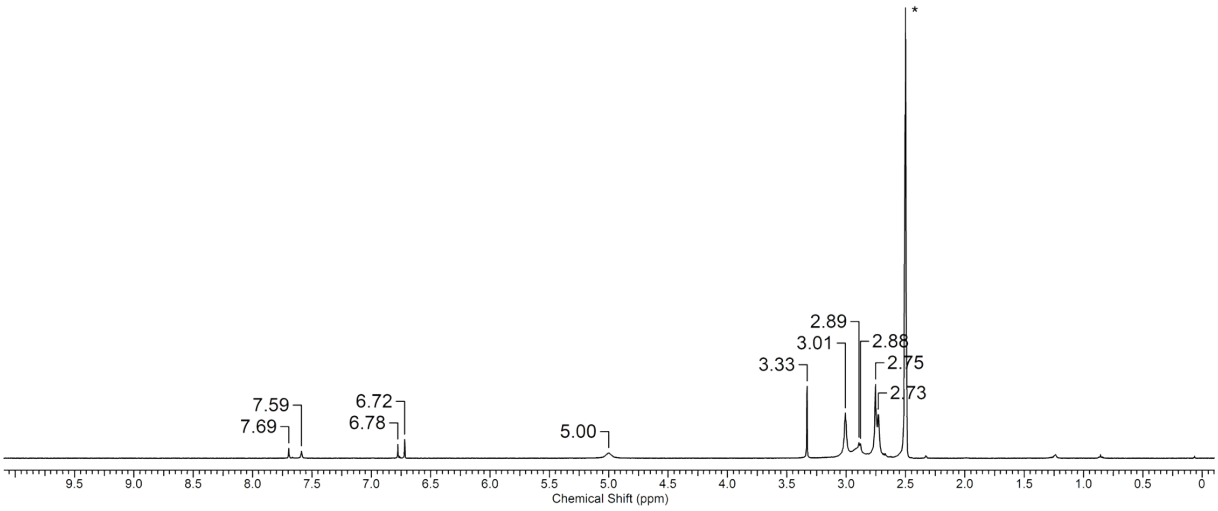

Figure S9 ^{1}H NMR (400 MHz) of [**1**+2(F_5Bn)]Br_2 dissolved in DMSO-d_6.

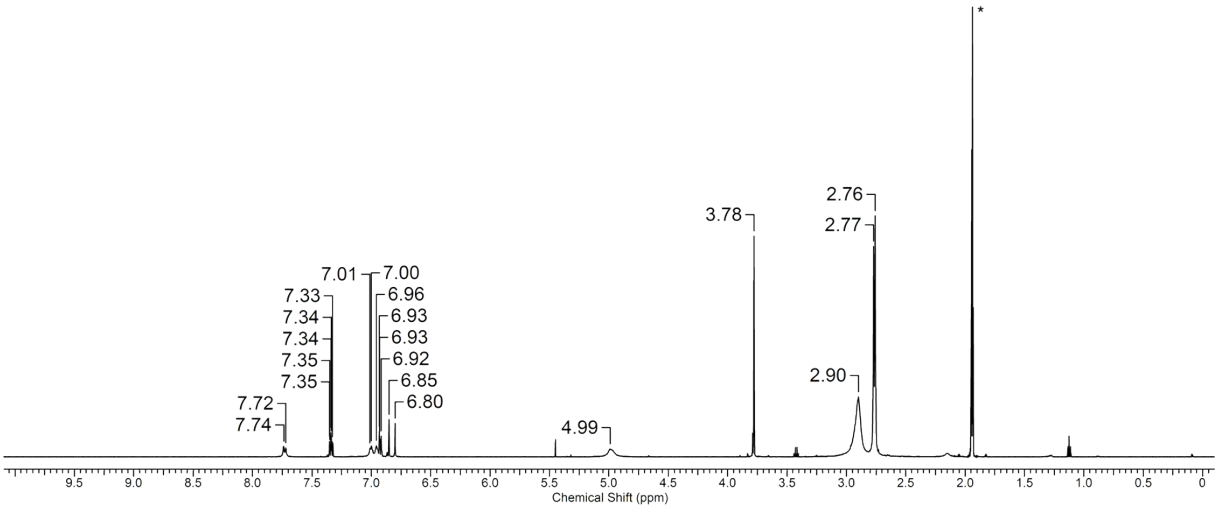

Figure S10 ^{1}H NMR (600 MHz) of [**1**+2(m-MeOBn)]Br_2 dissolved in CD_3CN.

Analytical data for [2+Bn]Br

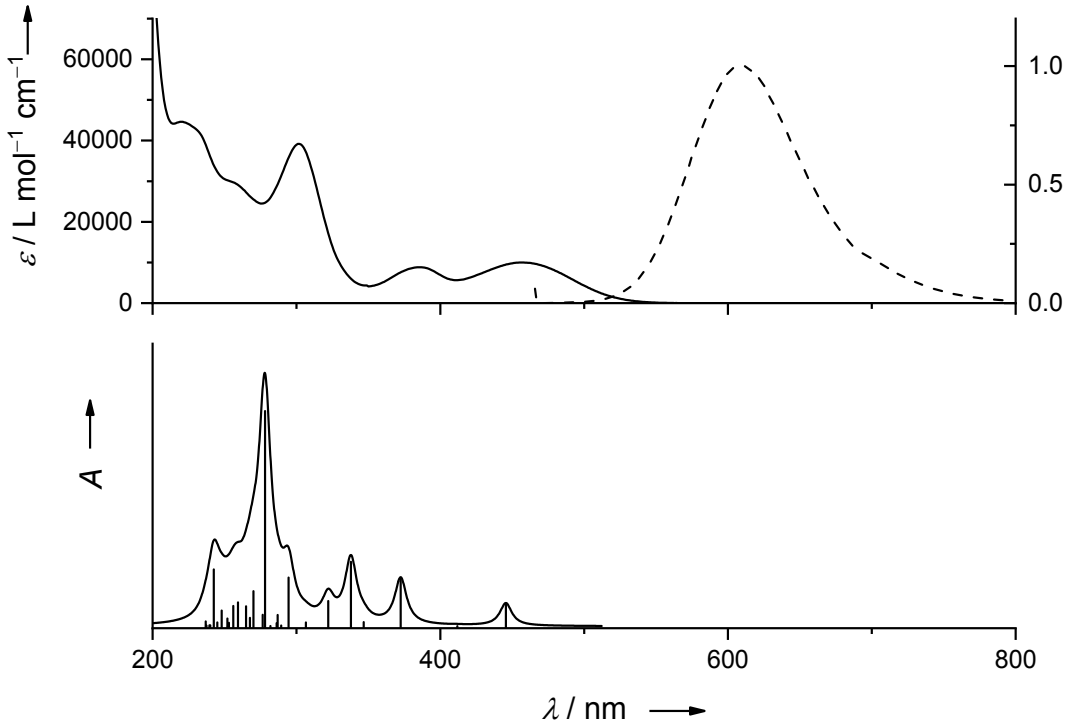

Figure S11 Electronic absorption and emission spactra (normalized) of [**2**+Bn]Br in CH_3CN and a simulation based on TD-DFT calculations at the B3LYP/TZVP level.

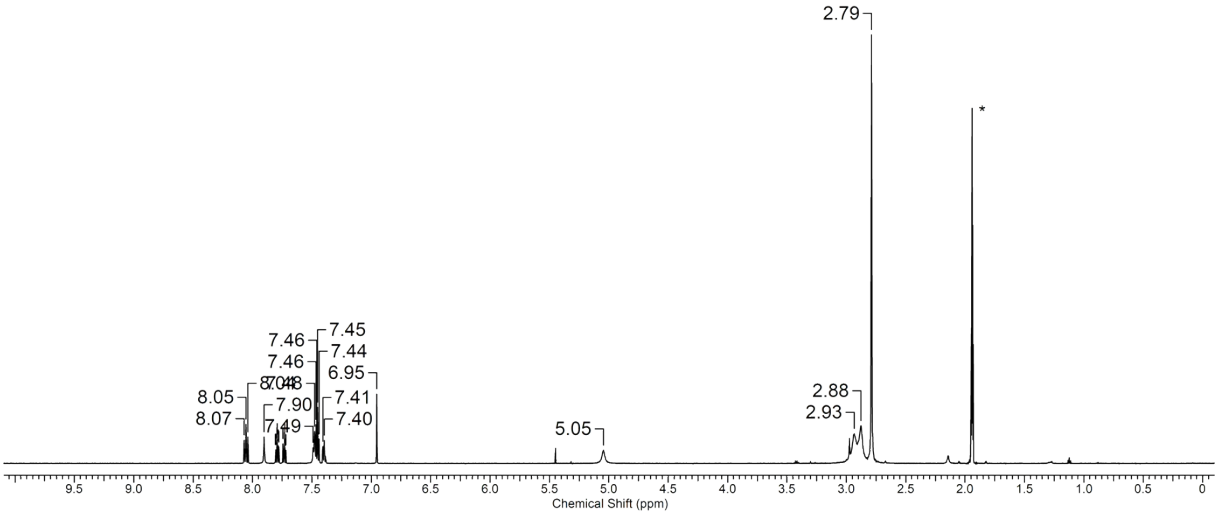

Figure S12 ^1H NMR spectrum (600 MHz) of [**2**+Bn]Br dissolved in CD_3CN.

EPR spectrum for [1$(CuCl_2)_2(CuCl)_2$]

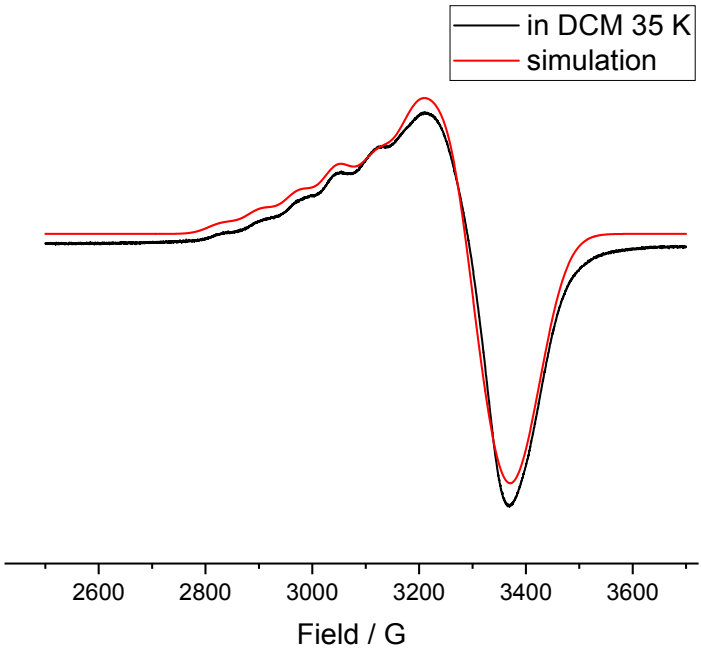

Figure S13 EPR spectrum of [**1**$(CuCl_2)_2(CuCl)_2$] in a frozen CH_2Cl_2 solution at 35 K. The fit was obtained with the following parameters: $g_{\parallel}$ = 2.258, $g_{\perp}$ = 2.072, $A_{\parallel}$ = 75 G, $A_{\perp}$ = 25 G.

Analytical data for [1(NiCl$_2$)$_2$(CuCl(CH$_3$CN))$_2$]

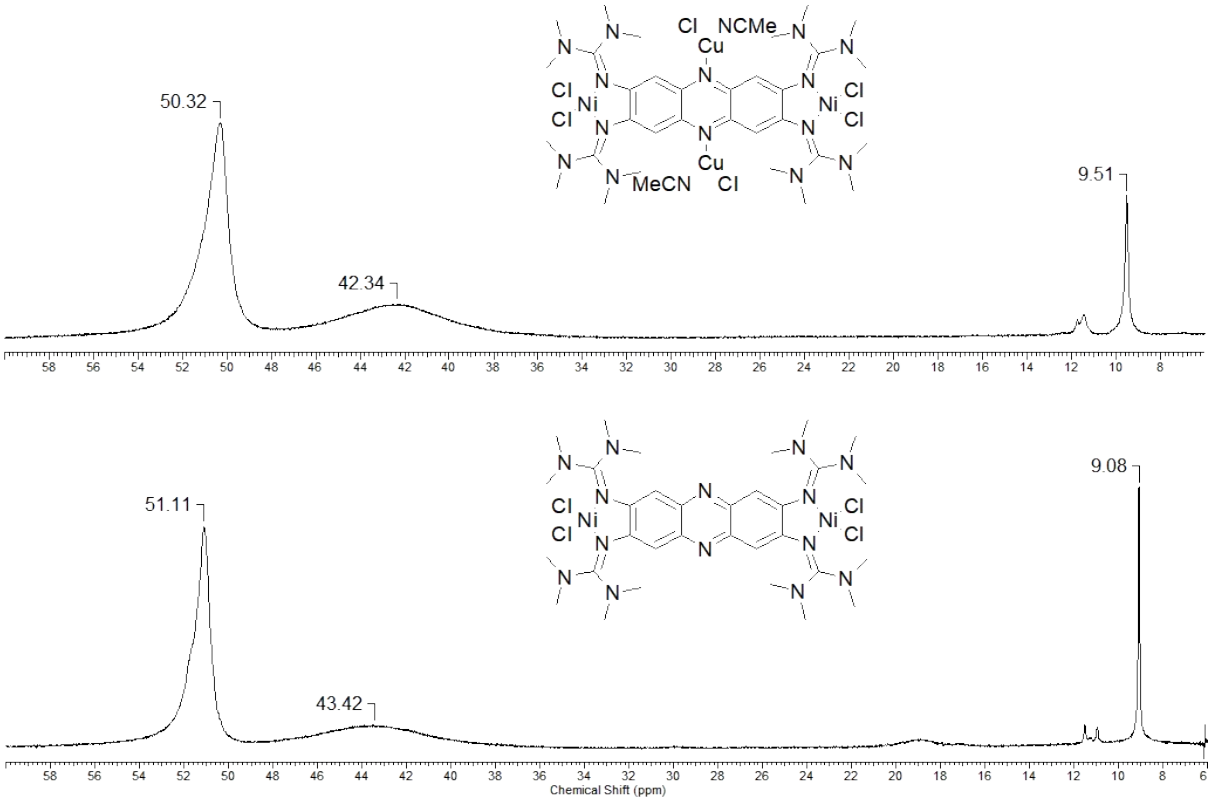

Figure S14 ^{1}H NMR spectra (200 MHz) of [**1**(NiCl$_2$)$_2$] (bottom) and [**1**(NiCl$_2$)$_2$(CuCl(CH$_3$CN))$_2$] (top) dissolved in CD$_3$CN.

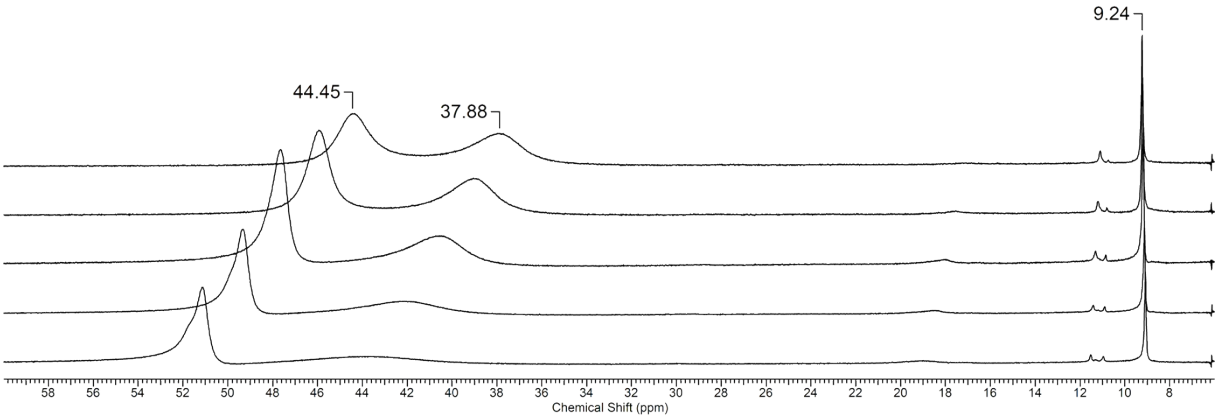

Figure S 15 Variable temperature ^{1}H NMR spectra from 300 to 340 K (from bottom to top) of [**1**(NiCl$_2$)$_2$] dissolved in CD$_3$CN.

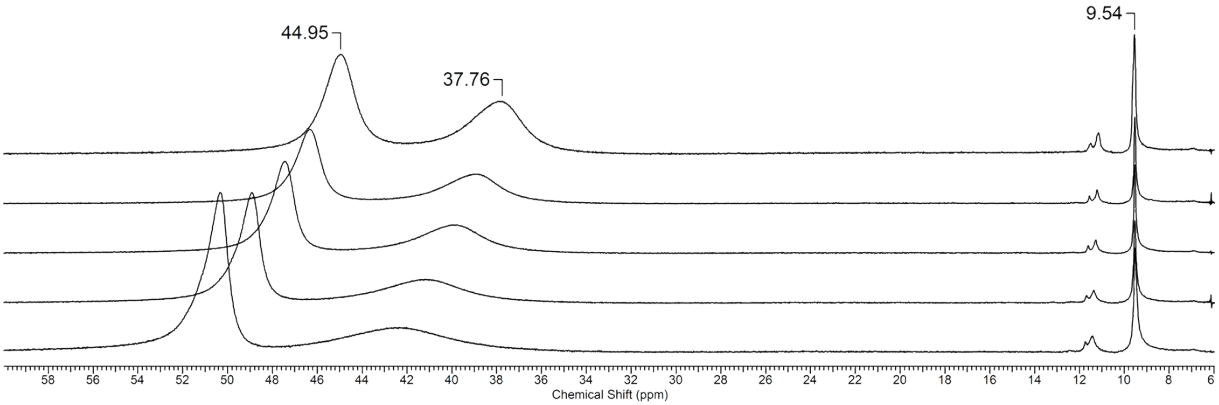

Figure S16 Variable temperature ^{1}H NMR spectra from 300 to 340 K (from bottom to top) of [**1**$(NiCl_2)_2(CuCl(CH_3CN))_2$] dissolved in CD_3CN.

Analytical data for [2($NiCl_2$)]

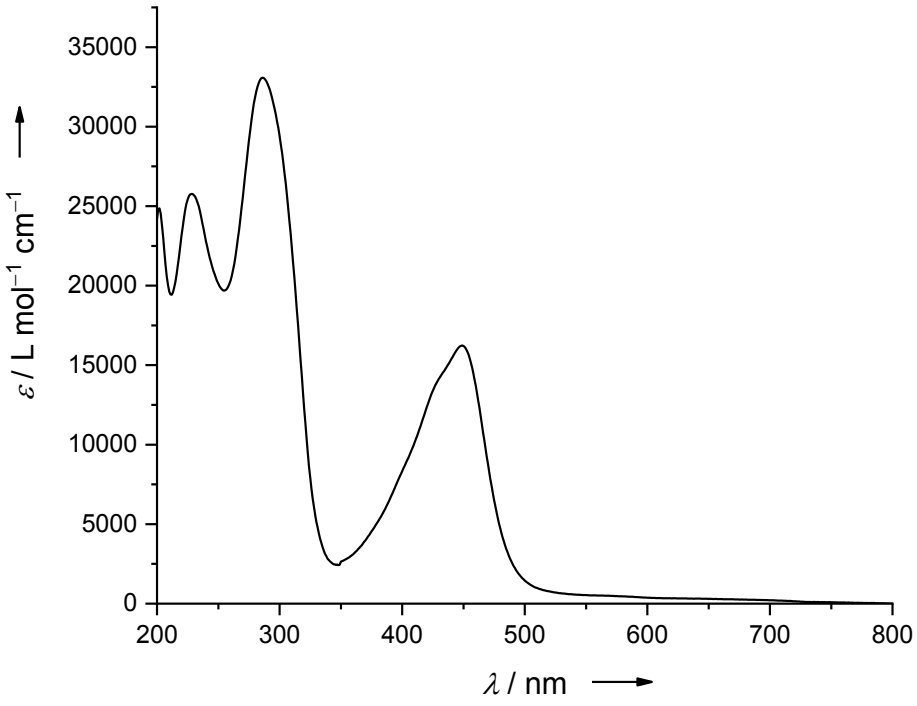

Figure S17 UV/Vis spectrum of [**2**($NiCl_2$)] dissolved in CH_3CN.

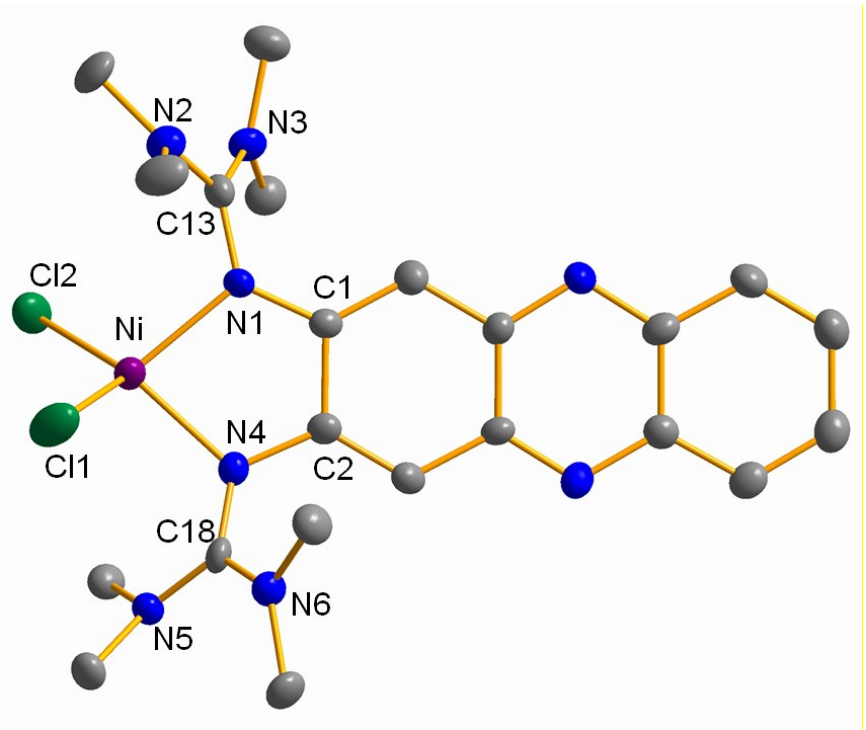

Figure S18 Structure of the complex [**2**($NiCl_2$)]. Vibrational ellipsoids drawn at the 50% probability level. Hydrogen atoms omitted for clarity. Selected structural parameters (bond distances in Å, angles in °): Ni-Cl1 2.2302(18), Ni-Cl2 2.2294(17), Ni-N1 1.991(4), Ni-N4 1.986(4), N1-C1 1.369(7), N1-C13 1.338(7), N4-C2 1.397(7), N4-C18 1.334(7), (Cl1-Ni-Cl2, N1-Ni-N4) 68.86.

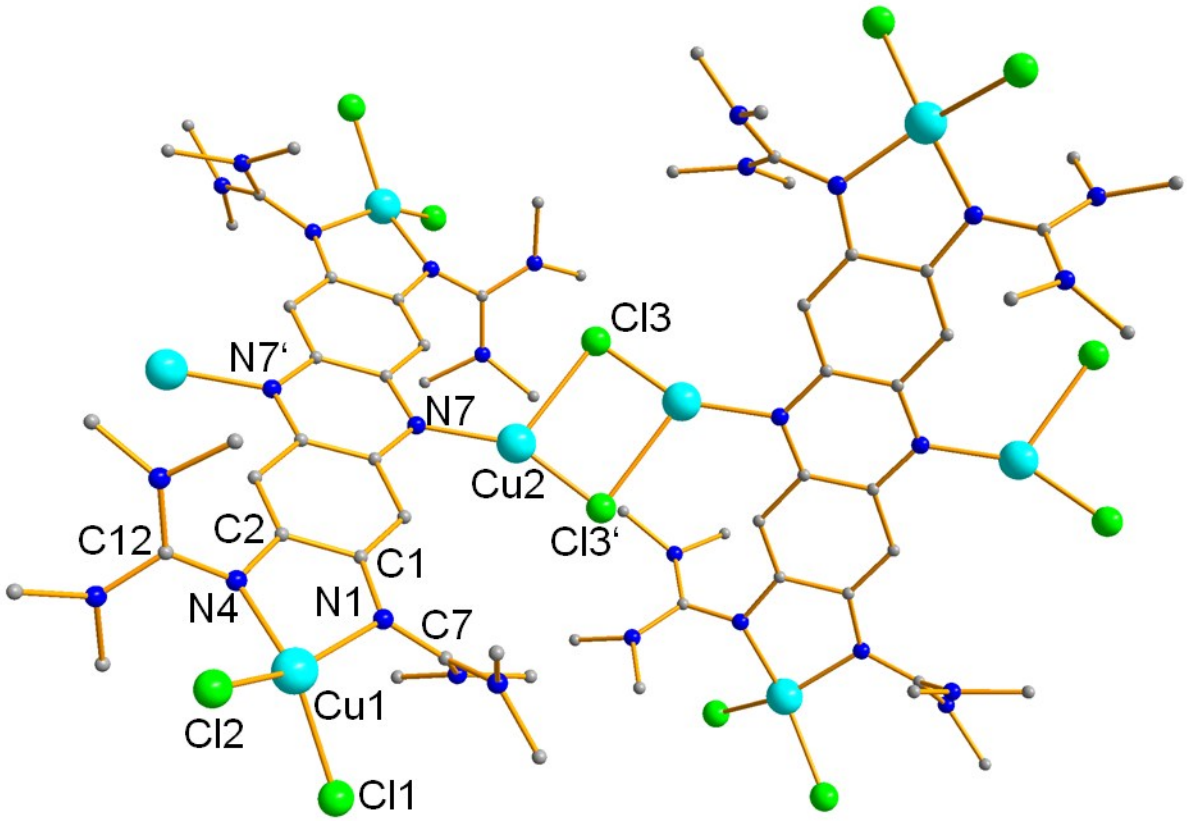

Figure S19 Section of the mixed-valent coordination polymer [**1**$(CuCl_2)_2(CuCl)_2]_n$. A ball-and-stick representation is shown. Hydrogen atoms omitted for clarity. Selected structural parameters (bond distances in Å, angles in °): Cu1-N1 1.987(4), Cu1-N4 1.964(4), Cu1-Cl1 2.2420(14), Cu1-Cl2 2.2265(15), Cu2-N7 1.981(5), Cu2-Cl3 2.102(3), Cu2-Cl3’ 2.669(3), N1-C1 1.388(6), N1-C7 1.342(6), N4-C2 1.368(7), N4-C12 1.329(7), N1-Cu1-N4 82.21(17), Cl1-Cu1-Cl2 99.45(6), N7-Cu2-Cl3 152.69(16), N7-Cu2-Cl3’ 118.33(15), Cl3-Cu-Cl3’ 88.88(9). Please note that the crystals were of bad quality. Therefore, the structural parameters are afflicted with a large error.

Crystal data: $C_{33.8}H_{55.6}Cl_{8.6}Cu_3N_{14}$: *M*r = 1153.61, 0.50 × 0.20 × 0.10 mm^3, monoclinic, space group *C*2/c, a = 21.862(4), b = 24.311(5), c = 14.152(3) Å, β = 117.18(3)°, V = 6691(3) $Å^3$, Z = 4, d_{calc} = 1.145 Mg m^{-3}, Mo-K_α radiation (l = 0.71073 Å), T = 100 K, θ_{range} 4.2 to 60.00°. Reflections measd. 55915, indep. 9742, R_{int} = 0.1217. Final R indices [I > 2s(I)]: R_1 = 0.0842, wR_2 = 0.2351.

SQUID data for [1(NiCl$_2$)$_2$]

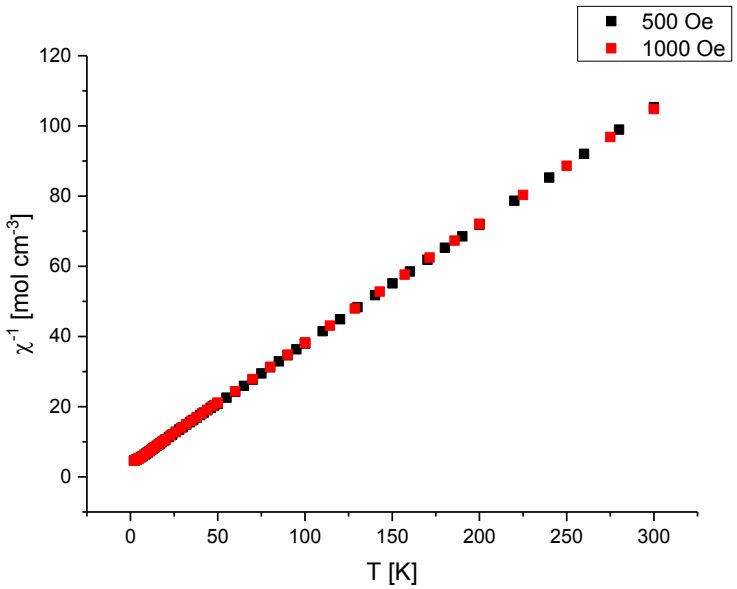

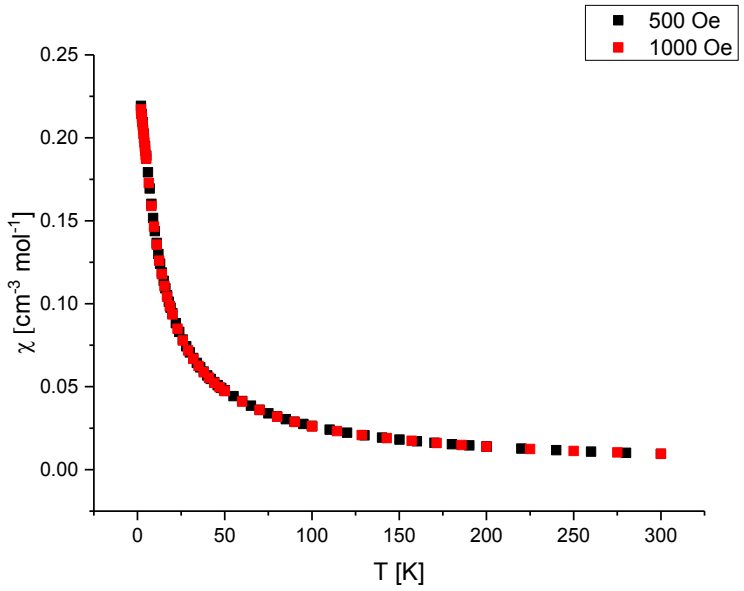

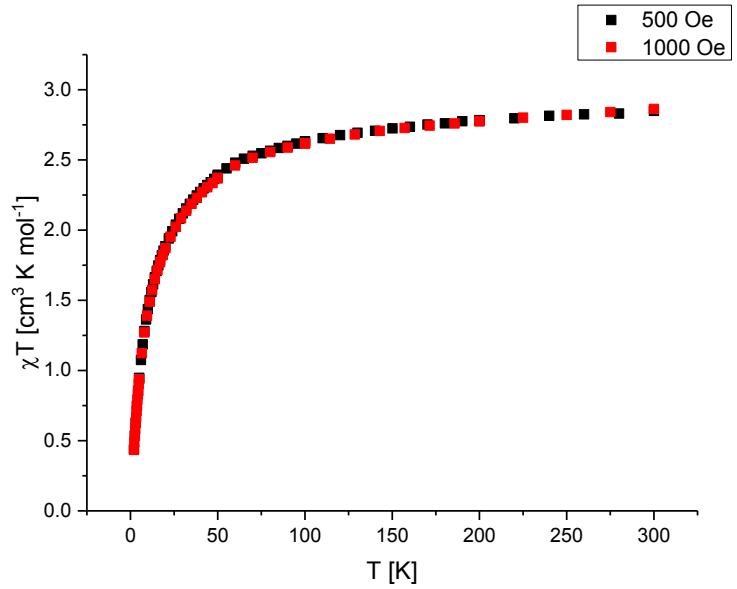
500 Oe
1000 Oe
χT [cm³ K mol⁻¹]
T [K]
0.0
0.5
1.0
1.5
2.0
2.5
3.0
0
50
100
150
200
250
300

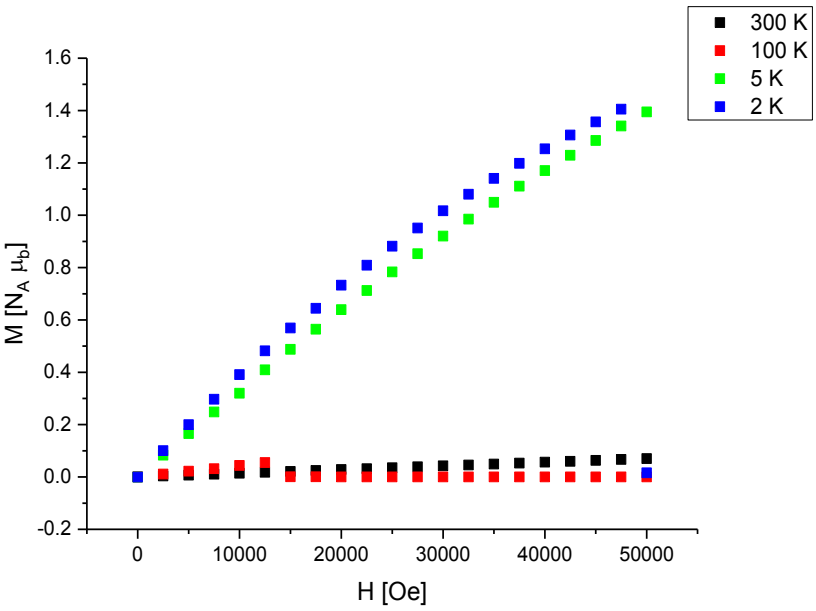
300 K
100 K
5 K
2 K
M [N_A μ_b]
H [Oe]
-0.2
0.0
0.2
0.4
0.6
0.8
1.0
1.2
1.4
1.6
0
10000
20000
30000
40000
50000

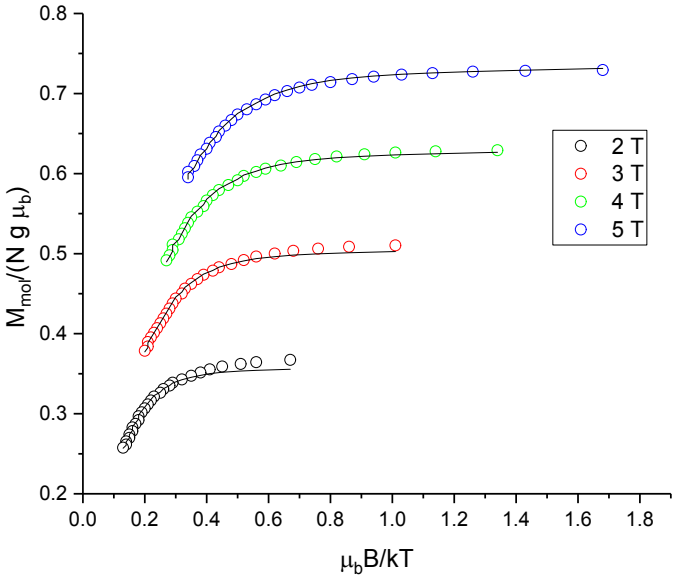

Fit parameters: J = 1.534; $g_1 = g_2$ = 2.07; $D_1 = D_2$ = 11.917; $E/D_1 = E/D_2$ = 2.091